

A LOW ENERGY ION BEAM PEPPER POT EMITTANCE DEVICE

M. Ripert, A.Buechel, A. Peters, J.Schreiner, T.Winkelmann, HIT, Heidelberg, Germany

Abstract

The transverse emittance of the ion beam at the Heidelberg Ion Therapy Center (HIT) will be measured within the Low Energy Beam Transport (LEBT) using a pepper-pot measurement system. At HIT, two ECR sources produce ions (H, He, C and O) at an energy of 8keV/u with different beam currents from about 80 μ A to 2mA. The functionality and components of the pepper-pot device is reviewed as well as the final design and the choice of the scintillator. For that, results from recent beam test at the Max Planck Institute für Kernphysik at Heidelberg are presented. The material investigation was focused on inorganic doped crystal, inorganic undoped crystal, borosilicate glass and quartz glass with the following characteristics: availability, prior use in beam diagnostics, radiation hardness, transparency, fast response, spectral matching to CCD detectors.

PEPPER POT DEVICE

Location

The Pepper-Pot Scintillator Screen system should fit within the existing beam line components (vacuum boxes already used with beam diagnostics equipment like Faraday cups, profile grids and slits). The N1DK1 vacuum box will be equipped with a fast iris shutter, a pepper-pot mask and a scintillator screen. The N1DK2 vacuum box will contain a 45 degrees tilted mirror inside and a CCD camera outside. (Figure 1)

The pepper-pot principle

The pepper-pot mask, which is perpendicular to the beam and contains a regular array of identical holes, splits the beam into beamlets. The scintillator is used to create a photographic image of the beamlets with pixel intensity corresponding to the charge concentration of beam particles striking the transparent scintillator. A CCD camera with a mirror placed behind at 45 degrees will record single and multi-shots.

Why using a pepper-pot device?

We want to measure both x-y components of the beam emittance simultaneously in one shot and to obtain data in real time. Four methods [1-2] can be used and all utilize a slit or mask to select a portion of the beam for analysis:

1. The two-slit scanner method uses a second slit which can be scanned through the direction parallel to the first. The cut out beam current is normally measured by a Faraday cup.

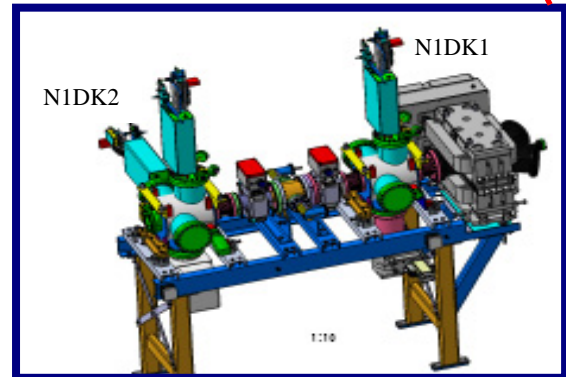
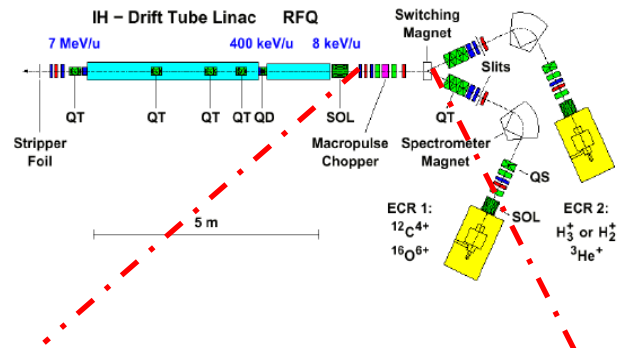


Figure 1: The Low Energy Beam Transport at HIT and the position of the Pepper-Pot Scintillator Screen device within the LEBT (Low Energy Beam Transfer).

However, this method is really slow because the second slit has to be scanned through the range for every position of the first slit.

2. With the multi-wire collector method, each wire collects the beam particles that pass through the slit. The disadvantage of this method is that it requires an amplifier for every wire in the collector.

3. The Allison-type emittance scanner is faster than the multi-wire collector method but slower than the pepper – pot method [2]

4. The Pepper-pot

Pepper pot measurement sequence and necessary components

Once the beam is tuned into the Faraday cup and a beam current measurement is acquired, the shutter (1) is released and the beam travels down to the pepper pot (2) mask (ideal case), and then to the scintillator screen (3).

The vacuum shutter UNIBLITZ VS35 [3] will be used. It has stainless steel blades, 35 mm aperture with a time to open of 13 ms. The pepper pot mask (60 mm*60 mm*0.1mm) is made of tungsten and should contain a 40*40 array hole with 50 μ m to 100 μ m holes diameter and 1 mm pitch). Since the range of 8 keV ions in tungsten is approximately 100 Angstrom, the tungsten will stop over 90 % of the ions. The holes will allow an ion beamlet to pass which then propagates through a distance of 15-100 mm. The beamlets then impinge on a scintillator screen (4). The screen should be 80*80 mm and resides on a fixed sample holder. Whereas the pepper pot mask resides on a sample holder driven by a linear rail. The mask should be movable from 15 mm to 100 mm (with respect to the screen). The mechanical design (figure 2) of the pepper-pot system is a collaboration between GSI and HIT.

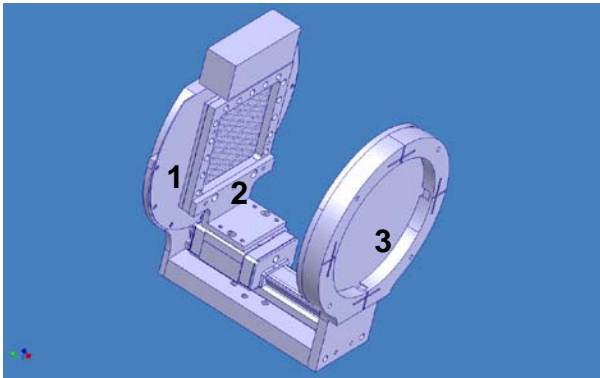


Figure 2: The Pepper-Pot Scintillator Screen bench. From left to right (1) shutter (2) pepper-pot mask (3) scintillator screen

SCINTILLATOR

The pepper pot mask and the measurement screen will be aligned perpendicularly to the beam. The beam images will be thus produced by a transparent scintillator and will be captured by a suitable CCD camera.

Why is the screen so important?

When the ion source delivers the beam to the pepper-pot, ideally, we would like the screen material to trap all coming particles and preserve the initial distribution over (x, x', y, y', E) . Could this information be corrupted while the material transmits photons?

The screen visualizes the beamlets. The dimension and the intensity distribution of the beamlets will then be correlated to the angular distribution. To enable high spatial resolution, the screen material should trap particles uniformly from a very broad distribution over x' and y' . In general, in most materials, particles are trapped uniformly.

The position coordinates (x, y) of the particles are generally preserved. The accuracy of the transmission in angles (x', y') should be one major point. Different type of scintillators could be used. Some of them have better light yield. That's why an experiment was performed with the collaboration of MPI-K to test the Light output, damage and reproducibility.

Properties

The materials, selected because of their availability, radiation hardness, transparency, fast response, prior use in beam diagnostics, or spectral matching to detectors (CCDs,...) are

- Inorganic Doped Crystal : YAG:Ce, YAP:Ce, Caf2:Eu (Crytur Inc.) [4]
- Inorganic Undoped Crystal : Sapphire, YAG (Focteck Inc) [5]
- Quartz : Herasil 3 & 102, Infrasil 301 & 302, Suprasil 1 & 300 (Aachener Quarz-Glas Technologie Heinrich) [6]
- Borosilicate Glass D 263 T (Präzisions Glas & Optik) [7]

One of the most important properties of fused quartz is its extremely low coefficient of expansion: $5.5 \cdot 10^{-7}$ mm $^{\circ}$ C. Its coefficient is 1/34 that of copper and only 1/7 of borosilicate glass. This makes the material particularly useful for applications which require local and minimum sensitivity to thermal changes.

Experiment at the Max Planck Institute - Heidelberg

These tests were made on the first week of November 2009. During these runs, the scintillator plate was placed in the beam path at a 45 degree angle and a CCD camera was recording images. Three scintillators could be placed on a holder and be tested with the same conditions in one machine run before breaking vacuum and replacing materials with three non-irradiated samples.

The ion beam parameters used in this experiment are the following:

- Ion Beam : protons
- Energy : 8 KeV/u
- Beam Current : 10 μ A
- Particles per pulse : $9.4 \cdot 10^{11}$ – $3 \cdot 10^{13}$
- Variable Pulse Length : 15 ms – 500 ms
- Frequency : 1 Hz

Each material is irradiated with 3 macro pulses of 15 ms, 20 ms,until 500 ms (or less if the light output intensity became constant) with a frequency of 1 Hz. At the end of the test a total irradiation time of 1.5 sec to 2 sec have been applied to each material.

The ion beam is first passing through a collimation entrance slits. Once the beam is tuned into the Faraday cup and a beam current measurement is acquired, the chopper is released and the beam travels down to the screen material situated in front of the Faraday Cup. In this way a flux up to 3×10^{13} pps for protons was achieved.

Three samples to be irradiated reside on a sample holder driven by a manual actuator (figure 3). The target is heated to below the melting point by the beam energy. The aim of this test was to evaluate the time dependence of the scintillating response of various scintillators.

Signal formation

The signal formation [8-9] of the scintillator light output consists of the following steps:

- Energy transfer from incident particles to secondary charged particles within the material. Charged particles being formed by the interaction of incident particles with the material.
- Energy transfer by secondary charged particles to luminescence centers [10]
- De-excitation of photons by excited luminescence centers which can lead to delayed fluorescence or phosphorescence (afterglow).
- Collection of photons by a CCD camera

Only a part of the incident energy lost within the material by the charged particles will become the excitation energy of the luminescence centers which will emit photons. Some multiple electronic excitations (electron-hole pairs) will be formed along the ion track. The electron-hole pairs resulting from the ionization process form separated charge defects that cause the surroundings atoms to rearrange themselves (relax). To reach electro-neutrality, holes and electrons will capture charge carriers. If the concentration of electrons and holes is inferior to the concentration of activator atoms, both holes and electrons will have a large probability to

be captured by different charge carriers. This recombination could generate electron centers (called F centers), hole centers (called H centers) and also self-trapped-hole centers (called V centers). For example, electrons in an F center will tend to absorb light in the visible such that the material becomes colored ("color center defect") which is defined as a slow recombination due to trapping (\sim ms). However, if an activator atom first captures one carrier, the result may be an electronic states of the activator atom or exciton which will be a considered a fast recombination.

The density of these defects (excitons, color centers) increases until large clusters of defects are formed which diffuse to the surface.

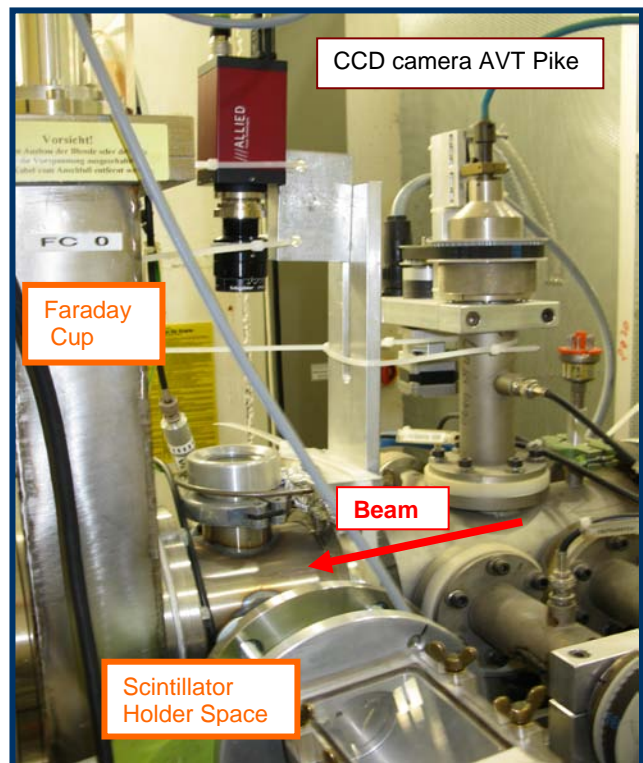


Figure 3: Ion Beam-Material Irradiation Test Setup at the Max-Planck Institute in Heidelberg.

Results

Matlab was used to process the images and to compute the intensity pixel values along the horizontal and vertical components.

Two groups can be categorized

- One with higher intensity values
- One with lower intensity values, two times lower than the first group.

The first group is primarily composed of the doped Inorganic Crystal: YAG:Ce, YAP:Ce and CaF₂:Eu. These crystals saturate from the beginning of the irradiation and

show some damage after being totally irradiated. Since the effect of saturation is intensity dependent, the use of YAG:Ce as a beam profile monitor should be limited to lower current densities for future experiment.

To gain in high temporal resolution, doped (Ce³⁺) scintillators with fast decay of light output and intensive fluorescence have been chosen. However, a fraction of scintillation light is still present a certain time after the excitation stops, which can be explained by two phenomena: delayed fluorescence or afterglow. Another fraction can also be seen before the intensive fluorescence making really inconvenient the possibility to measure the light output for a specific irradiation time (and for the total irradiation) and the repeatability of the measurement. As seen in figure 5 A-B, the intensity profile for 40 ms shows some large discrepancy in the repeatability of the light output.

A decrease of the optical transmission which causes a decrease in the intensity distribution can also deteriorate the spatial resolution. An example of this damage can be seen in figure 5-A where a part of the horizontal intensity profile of YAG:Ce disappears slowly with time. In figure 4-B, the damage “blackened” area has been revealed thanks to a 10 pA beam current. After a total irradiation of 2000 ms, one part of YAG:Ce cannot scintillate anymore due to some degradation. However, a standard microscope does not show any damage (burning bubbles, changes in colour...)

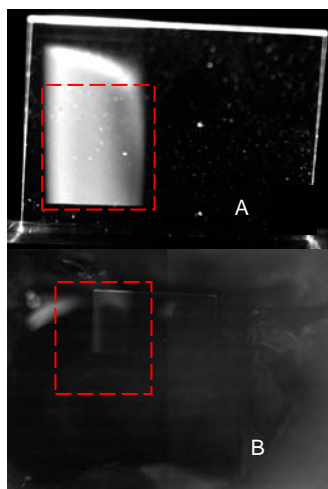


Figure 4 A-B: The degradation of YAG:Ce after a total irradiation of 2000 ms (which is equivalent to $1.4 \cdot 10^{14}$ particle per pulse) can be seen in picture B.

The second group shows also some materials with some distorted Gaussian beam profile over the horizontal axis and some saturation effect over the y axis.

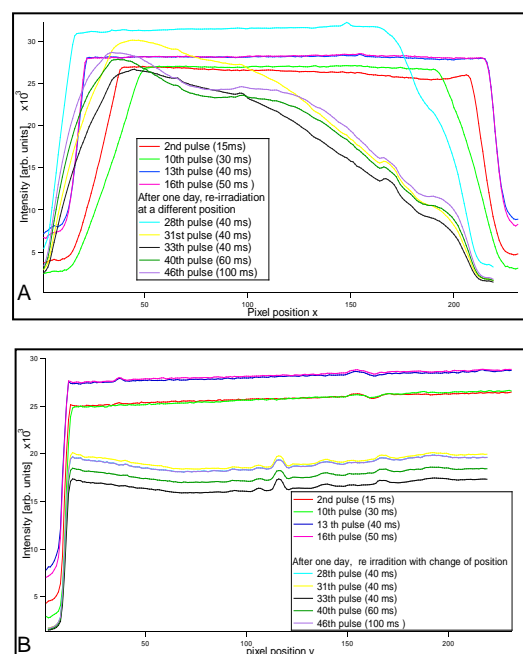


Figure 5 A-B: The intensity distribution of image 4 A is plotted over the horizontal (A) and vertical (B).

For sapphire, the light output increases with the integrated beam pulse but still lead to some damaging effect “blackening”. The YAG undoped shows some similar behaviour which results in some damage after a total irradiation time of 1.3 seconds. (Figure 6) This picture confirms that undoped material cannot be used anymore. Only a small part of the material scintillates, a big part (corresponding to the irradiated beam width of the previous day) does not scintillate at all.

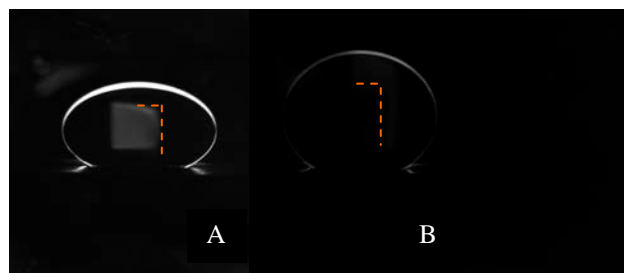


Figure 6: Degradation Effects of undoped YAG after an integrated irradiation time of 1.3 seconds.

Borosilicatte Glass and Suprasil 300 demonstrate some really low light output and some fluctuations in the intensity distribution with respect to the beam pulse. Consequently, repeatability of the measurement could not be achieved.

Between this two groups, Herasil 3, Infrasil 302 and Suprasil 1 could be of some interest. The light output of

these scintillators is sufficient and increases with the beam pulses (Figure 7).

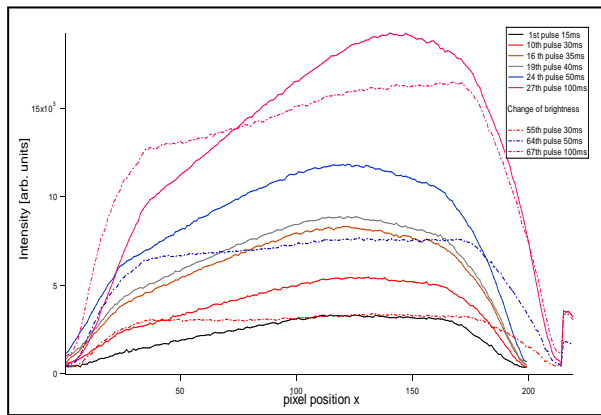


Figure 7 : The repeatability of the intensity distribution over 65 beam pulse of Herasil 3 (which is equivalent to a integrated time of ~ 2000 ms) and the degradation effects after changing the CCD camera set-up to a lower brightness

In the experiment, an image was taken of the material irradiation every 1 Hz (for three beam macro pulses). The beam pulse is then increased until 200ms. Afterwards, a change in the CCD parameters (lowering brightness level) lead to another set of images taken with the same beam parameter setting (energy, current ...) and without breaking the vacuum. The repeatability of these measurements is shown in the figure 6. The light output distribution for Herasil 3 is shown from the 1st to the 65th pulses. The new set of data (after the change of parameters of the CCD camera) for different beam pulse shows the same phenomenon: their corresponding intensity distribution follows the “previous” data curve until the distribution broke. The “flat top” appearing after ~ 100 ms of integrated irradiation can be due to saturation of activator centers, slow decay processes (slow recombination due to trapping), or some non- visible damage. The same behavior can be seen for Suprasil 1 and Infrasil 302.

Most of the materials except the doped inorganic crystal have a “flat top” distribution in the vertical axis and a “broken” non Gaussian distribution in the horizontal axis from the beginning of the irradiation. This distribution is not homogeneous and this pattern was also observed when increasing the irradiation time. A longer irradiation time did not lead to a more homogeneous intensity distribution for most of them. These heterogeneities can be due to the beam delivery or to the non-homogeneity of the crystal. Such effects should be investigated by studying the relationships between the beam parameters and the achieved effects.

The decrease of light output can be due to the saturation of activation centers, the slow decay processes, and also

some damage. Due to the existence of slow decay processes which are mainly caused by charge carrier re-trapping at shallow traps, the light output does not increase with respect to the integration time. Additionally, some large fluctuation of the intensity distribution has been observed. However, in order to explain the slower scintillation process in the timescale of ms and these large fluctuations, such effects should be investigated.

CONCLUSION

The design of the pepper pot mechanics is completed and is under construction. The pepper pot device will be implemented at HIT in a new research and development test bench available in September 2010.

The inorganic doped scintillators have a greater light output than the inorganic undoped scintillator and the quartz material. However, some aspects of their scintillation behaviour (large fluctuations of their light output, non-repeatability of measurement) have not been explained satisfactorily and need further investigation.

ACKNOWLEDGMENTS

I would like to thank Manfred Köning of MPI-K for the assistance in running the accelerator, and to Christoph Dorn of GSI for the mechanical design. Thanks also go to Tim Winkelmann for assistance in running the test at MPI-K. It is a pleasure to acknowledge helpful discussions with Christophe Dujardin, Ayman S. El-Said, Rainer Haseitl, Simon Jolly, Erik Ritter, Markus Strohmeier, Richard Wihelm. This work is funded by the European commission as part of the FP7 Marie Curie Actions under contract number PITN-GA-215080.

REFERENCES

- [1] T.Hoffmann, W.Barth, P.Forck, A.Peters, P.Strehl , Emittance Measurements of High Current Heavy Io Beams Using a Single Shot Pepper pot System
- [2] M.P.Stockli et al, Measuring and Analysing Transverse Emittances of Charged Particle Beams, BIW'06, Batavia, IL, 2006, AIP Conf. Proc.868, p.25.
- [3] Uniblitz Inc, from <http://www.uniblitz.com/>
- [4] Crytur Ltd, from <http://www.crytur.com/>
- [5] Foctek Photonics Inc, from <http://www.foctek.net/>
- [6] Aachener Quarz-Glas Technologie Heinrich, from <http://www.quarzglas-heinrich.de/>
- [7] Präzisions Glas & Optik, from <http://www.pgo-online.com/intl/>
- [8] R.B.Murray; A.Meyer, Phys.Rev. 122(1961) 815
- [9] J.A.Mares et al.,IEEE transactions on nuclear science, vol 55, No.3, June 2008
- [10] T. J. Renk et al., Proceedings of the IEEE, 92, No. 7, 1057–1081 (2004)